science for a changing world

Techniques of Water-Resources Investigations of the United States Geological Survey

Chapter A4

A MODULAR FINITE-ELEMENT MODEL (MODFE) FOR AREAL AND AXISYMMETRIC GROUND-WATER FLOW PROBLEMS, PART 2: DERIVATION OF FINITE-ELEMENT EQUATIONS AND COMPARISONS WITH ANALYTICAL SOLUTIONS

By Richard L. Cooley

Book 6
Chapter A4

U.S. DEPARTMENT OF THE INTERIOR
MANUEL LUJAN, Jr., *Secretary*

U.S. GEOLOGICAL SURVEY
Dallas L. Peck, *Director*

UNITED STATES GOVERNMENT PRINTING OFFICE: 1992

For sale by Book and Open-File Report Sales, U.S. Geological Survey,
Federal Center, Box 25425, Denver, CO 80225

PREFACE

The series of manuals on techniques describes procedures for planning and executing specialized work in water-resources investigations. The material is grouped under major subject headings called "Books" and further subdivided into sections and chapters. Section A of Book 6 is on ground-water modeling.

The unit of publication, the chapter, is limited to a narrow field of subject matters. This format allows flexibility in revision and publication as the need arises. Chapters 6A3, 6A4, and 6A5 are on the use of a particular transient finite-element numerical method for two-dimensional ground-water flow problems. These Chapters (6A3, 6A4, and 6A5) correspond to reports prepared on the finite-element model given the acronym MODFE and designated as parts 1, 2, and 3, respectively. Part 1 is on "model description and user's manual," part 2 is on "derivation of finite-element equations and comparisons with analytical solutions," and part 3 is on "design philosophy and programming details." Parts 1 and 3 have been released as Open-File Reports (see References, Torak (1992 a, b)) pending publication as Chapters 6A3 and 6A5 respectively.

TECHNIQUES OF WATER-RESOURCES INVESTIGATIONS OF THE U.S. GEOLOGICAL SURVEY

The U.S. Geological Survey publishes a series of manuals describing procedures for planning and conducting specialized work in water-resources investigations. The manuals published to date are listed below and may be ordered by mail from the **U.S. Geological Survey, Books and Open-File Reports Section, Federal Center, Box 25425, Denver, Colorado 80225** (an authorized agent of the Superintendent of Documents, Government Printing Office).

Prepayment is required. Remittance should be sent by check or money order payable to U.S. Geological Survey. Prices are not included in the listing below as they are subject to change. **Current prices can be obtained** by writing to the USGS address shown above. Prices include cost of domestic surface transportation. For transmittal outside the U.S.A. (except to Canada and Mexico) a surcharge of 25 percent of the net bill should be included to cover surface transportation. When ordering any of these publications, please give the title, book number, chapter number, and "U.S. Geological Survey Techniques of Water-Resources Investigations."

TWRI 1–D1. Water temperature—influential factors, field measurement, and data presentation, by H.H. Stevens, Jr., J.F. Ficke, and G.F. Smoot. 1975. 65 pages.
TWRI 1–D2. Guidelines for collection and field analysis of ground-water samples for selected unstable constituents, by W.W. Wood. 1976. 24 pages.
TWRI 2–D1. Application of surface geophysics to ground-water investigations, by A.A.R. Zohdy, G.P. Eaton, and D.R. Mabey. 1974. 116 pages.
TWRI 2–D2. Application of seismic-refraction techniques to hydrologic studies, by F.P. Haeni. 1988. 86 pages.
TWRI 2–E1. Application of borehole geophysics to water-resources investigations, by W.S. Keys and L.M. MacCary. 1971. 126 pages.
TWRI 2–E2. Borehole geophysics applied to ground-water investigations, by W. Scott Keys. 1990. 150 pages.
TWRI 2–F1. Application of drilling, coring, and sampling techniques to test holes and wells, by Eugene Shuter and Warren E. Teasdale. 1989. 97 pages.
TWRI 3–A1. General field and office procedures for indirect discharge measurements, by M.A. Benson and Tate Dalrymple. 1967. 30 pages.
TWRI 3–A2. Measurement of peak discharge by the slope-area method, by Tate Dalrymple and M.A. Benson. 1967. 12 pages.
TWRI 3–A3. Measurement of peak discharge at culverts by indirect methods, by G.L. Bodhaine. 1968. 60 pages.
TWRI 3–A4. Measurement of peak discharge at width contractions by indirect methods, by H.F. Matthai. 1967. 44 pages.
TWRI 3–A5. Measurement of peak discharge at dams by indirect methods, by Harry Hulsing. 1967. 29 pages.
TWRI 3–A6. General procedure for gaging streams, by R.W. Carter and Jacob Davidian. 1968. 13 pages.
TWRI 3–A7. Stage measurements at gaging stations, by T.J. Buchanan and W.P. Somers. 1968. 28 pages.
TWRI 3–A8. Discharge measurements at gaging stations, by T.J. Buchanan and W.P. Somers. 1969. 65 pages.
TWRI 3–A9.[1] Measurement of time of travel in streams by dye tracing, by F.A. Kilpatrick and J.F. Wilson, Jr. 1989. 27 pages.
TWRI 3–A10. Discharge ratings at gaging stations, by E.J. Kennedy. 1984. 59 pages.
TWRI 3–A11. Measurement of discharge by moving-boat method, by G.F. Smoot and C.E. Novak. 1969. 22 pages.
TWRI 3–A12. Fluorometric procedures for dye tracing, Revised, by J.F. Wilson, Jr., E.D. Cobb, and F.A. Kilpatrick. 1986. 41 pages.
TWRI 3–A13. Computation of continuous records of streamflow, by E.J. Kennedy. 1983. 53 pages.
TWRI 3–A14. Use of flumes in measuring discharge, by F.A. Kilpatrick, and V.R. Schneider. 1983. 46 pages.
TWRI 3–A15. Computation of water-surface profiles in open channels, by Jacob Davidian. 1984. 48 pages.
TWRI 3–A16. Measurement of discharge using tracers, by F.A. Kilpatrick and E.D. Cobb. 1985. 52 pages.
TWRI 3–A17. Acoustic velocity meter systems, by Antonius Laenen. 1985. 38 pages.
TWRI 3–A18. Determination of stream reaeration coefficients by use of tracers, by F.A. Kilpatrick, R.E. Rathbun, N. Yotsukura, G.W. Parker, and L.L. DeLong. 1989. 52 pages.
TWRI 3–A19. Levels at streamflow gaging stations, by E.J. Kennedy. 1990. 31 pages.
TWRI 3–B1. Aquifer-test design, observation, and data analysis, by R.W. Stallman. 1971. 26 pages.
TWRI 3–B2.[2] Introduction to ground-water hydraulics, a programmed text for self-instruction, by G.D. Bennett. 1976. 172 pages.

---

[1]This manual is a revision of "Measurement of Time of Travel and Dispersion in Streams by Dye Tracing," by E.F. Hubbard, F.A. Kilpatrick, L.A. Martens, and J.F. Wilson, Jr., Book 3, Chapter A9, published in 1982.
[2]Spanish translation also available.

TWRI 3–B3. Type curves for selected problems of flow to wells in confined aquifers, by J.E. Reed. 1980. 106 pages.
TWRI 3–B4. Regression modeling of ground-water flow, by Richard L. Cooley and Richard L. Naff. 1990. 232 pages.
TWRI 3–B5. Definition of boundary and initial conditions in the analysis of saturated ground-water flow systems—An introduction, by O. Lehn Franke, Thomas E. Reilly, and Gordon D. Bennett. 1987. 15 pages.
TWRI 3–B6. The principle of superposition and its application in ground-water hydraulics, by Thomas E. Reilly, O. Lehn Franke, and Gordon D. Bennett. 1987. 28 pages.
TWRI 3–B7. Analytical solutions for one-, two-, and three-dimensional solute transport in ground-water systems with uniform flow, by Eliezer J. Wexler. 1991. 193 pages.
TWRI 3–C1. Fluvial sediment concepts, by H.P. Guy. 1970. 55 pages.
TWRI 3–C2. Field methods of measurement of fluvial sediment, by H.P. Guy and V.W. Norman. 1970. 59 pages.
TWRI 3–C3. Computation of fluvial-sediment discharge, by George Porterfield. 1972. 66 pages.
TWRI 4–A1. Some statistical tools in hydrology, by H.C. Riggs. 1968. 39 pages.
TWRI 4–A2. Frequency curves, by H.C. Riggs, 1968. 15 pages.
TWRI 4–B1. Low-flow investigations, by H.C. Riggs. 1972. 18 pages.
TWRI 4–B2. Storage analyses for water supply, by H.C. Riggs and C.H. Hardison. 1973. 20 pages.
TWRI 4–B3. Regional analyses of streamflow characteristics, by H.C. Riggs. 1973. 15 pages.
TWRI 4–D1. Computation of rate and volume of stream depletion by wells, by C.T. Jenkins. 1970. 17 pages.
TWRI 5–A1. Methods for determination of inorganic substances in water and fluvial sediments, by Marvin J. Fishman and Linda C. Friedman, editors. 1989. 545 pages.
TWRI 5–A2. Determination of minor elements in water by emission spectroscopy, by P.R. Barnett and E.C. Mallory, Jr. 1971. 31 pages.
TWRI 5–A3.[1] Methods for the determination of organic substances in water and fluvial sediments, edited by R.L. Wershaw, M.J. Fishman, R.R. Grabbe, and L.E. Lowe. 1987. 80 pages.
TWRI 5–A4.[2] Methods for collection and analysis of aquatic biological and microbiological samples, by L.J. Britton and P.E. Greeson, editors. 1989. 363 pages.
TWRI 5–A5. Methods for determination of radioactive substances in water and fluvial sediments, by L.L. Thatcher, V.J. Janzer, and K.W. Edwards. 1977. 95 pages.
TWRI 5–A6. Quality assurance practices for the chemical and biological analyses of water and fluvial sediments, by L.C. Friedman and D.E. Erdmann. 1982. 181 pages.
TWRI 5–C1. Laboratory theory and methods for sediment analysis, by H.P. Guy. 1969. 58 pages.
TWRI 6–A1. A modular three-dimensional finite-difference ground-water flow model, by Michael G. McDonald and Arlen W. Harbaugh. 1988. 586 pages.
TWRI 6–A2. Documentation of a computer program to simulate aquifer-system compaction using the modular finite-difference ground-water flow model, by S.A. Leake and D.E. Prudic. 1991. 68 pages.
TWRI 6–A4. A modular finite-element model (MODFE) for areal and axisymmetric ground-water flow problems, Part 2: Derivation of finite-element equations and comparisons with analytical solutions, by R.L. Cooley. 1992. 108 pages.
TWRI 7–C1. Finite difference model for aquifer simulation in two dimensions with results of numerical experiments, by P.C. Trescott, G.F. Pinder, and S.P. Larson. 1976. 116 pages.
TWRI 7–C2. Computer model of two-dimensional solute transport and dispersion in ground water, by L.F. Konikow and J.D. Bredehoeft. 1978. 90 pages.
TWRI 7–C3. A model for simulation of flow in singular and interconnected channels, by R.W. Schaffranek, R.A. Baltzer, and D.E. Goldberg. 1981. 110 pages.
TWRI 8–A1. Methods of measuring water levels in deep wells, by M.S. Garber and F.C. Koopman. 1968. 23 pages.
TWRI 8–A2. Installation and service manual for U.S. Geological Survey monometers, by J.D. Craig. 1983. 57 pages.
TWRI 8–B2. Calibration and maintenance of vertical-axis type current meters, by G.F. Smoot and C.E. Novak. 1968. 15 pages.

---

[1]This manual is a revision of TWRI 5–A3, "Methods of Analysis of Organic Substances in Water," by Donald F. Goerlitz and Eugene Brown, published in 1972.

[2]This manual supersedes TWRI 5–A4, "Methods for collection and analysis of aquatic biological and microbiological samples," edited by P.E. Greeson and others, published in 1977.

CONTENTS

FIGURES

A MODULAR FINITE-ELEMENT MODEL (MODFE) FOR AREAL AND AXISYMMETRIC GROUND-WATER FLOW PROBLEMS, PART 2: DERIVATION OF FINITE-ELEMENT EQUATIONS AND COMPARISONS WITH ANALYTICAL SOLUTIONS

By Richard L. Cooley

ABSTRACT

MODFE, a modular finite-element model for simulating steady- or unsteady-state, areal or axisymmetric flow of ground water in a heterogeneous anisotropic aquifer is documented in a three-part series of reports. In this report, part 2, the finite-element equations are derived by minimizing a functional of the difference between the true and approximate hydraulic head, which produces equations that are equivalent to those obtained by either classical variational or Galerkin techniques. Spatial finite elements are triangular with linear basis functions, and temporal finite elements are one dimensional with linear basis functions. Physical processes that can be represented by the model include (1) confined flow, unconfined flow (using the Dupuit approximation), or a combination of both; (2) leakage through either rigid or elastic confining units; (3) specified recharge or discharge at points, along lines, or areally; (4) flow across specified-flow, specified-head, or head-dependent boundaries; (5) decrease of aquifer thickness to zero under extreme water-table decline and increase of aquifer thickness from zero as the water table rises; and (6) head-dependent fluxes from springs, drainage wells, leakage across riverbeds or confining units combined with aquifer dewatering, and evapotranspiration.

The matrix equations produced by the finite-element method are solved by the direct symmetric-Doolittle method or the iterative modified incomplete-Cholesky conjugate-gradient method. The direct method can be efficient for small- to medium-sized problems (less than about 500 nodes), and the iterative method is generally more efficient for larger-sized problems. Comparison of finite-element solutions with analytical solutions for five example problems demonstrates that the finite-element model can yield accurate solutions to ground-water flow problems.

INTRODUCTION

This report is the second part of a three-part series of reports (parts 1 and 3 are by Torak, 1992a and 1992b) that document the computer program MODFE (modular finite-element model), which simulates steady- or unsteady-state, areal or axisymmetric flow of ground water in a heterogeneous, anisotropic aquifer. The model incorporates a variety of physical processes necessary to simulate ground-water flow in the complicated settings that often characterize actual field problems. Flow may be confined, unconfined (using the Dupuit assumption), or a combination of both; known recharge and discharge may be distributed areally, along lines such as specified-flow boundaries, or at point sources and sinks such as pumping wells; and head-dependent leakage may be distributed areally, such as through confining units or wide riverbeds, or along lines such as narrow riverbeds. Confining units may be rigid or may have elastic storage capacity. Special nonlinear, head-dependent source and sink functions allow simulation of springs, drainage wells, rivers or confining units combined with aquifer dewatering, and evapotranspiration.

The material in the three reports has evolved over the past 10 years from material presented by the authors in the courses entitled "Finite-Element Modeling of Ground-Water Flow" held at the U.S. Geological Survey National Training Center in Denver, Colorado. These reports formalize the course material and incorporate valuable suggestions and comments from attendees of the courses.

Features that appear to be new, at least to published finite-element programs for ground-water flow, include (1) the method of deriving the finite-element equations from a functional of the difference between the true and approximate solutions, (2) the method of approximating the variability of transmissivity over an element so that the coefficient matrix does not have to be reassembled element by element each time the saturated thickness changes, (3) the method of treating decreases of aquifer thickness to zero under conditions of extreme water-table decline and increases of aquifer thickness from zero as the water-table rises, (4) the finite-element in time method for deriving (a) the finite-element equations for unconfined flow and (b) the functions for nonlinear, head-dependent sources and sinks, and (5) the method for incorporating transient leakage from confining units.

PURPOSE AND SCOPE

The purpose of this second part of the three-part series of reports is to derive the finite-element equations for the physical processes contained in the finite-element model. A knowledge of the physics of ground-water flow, as explained by Bear (1979), for example, is assumed. The differential equations that describe the physics of the flow processes are stated and the situations under which they apply are briefly explained, but the equations are not derived here. Basic differential and integral calculus and the symbolic representation of systems of equations using matrix algebra are used extensively.

This report is organized as follows. First, the basic differential equation and boundary conditions for unsteady-state flow in a confined aquifer are stated and the finite-element equations for this system are derived in Cartesian coordinates. Next, the finite-element equations are extended to include unconfined or combined confined and unconfined flow; decreases of aquifer thickness to zero and increases from zero; the nonlinear, head-dependent source and sink functions; and transient leakage from confining units. Following this, finite-element equations are derived in axisymmetric cylindrical coordinates and in steady-state form for either areal or axisymmetric problems. Finally, two matrix solution procedures are presented: a direct factorization method and an iterative, generalized conjugate-gradient procedure combined with approximate factorization.

Symbols used are defined where they first appear and in a special notation section at the end of the report. This should minimize confusion over use of similar symbols in different contexts.

ACKNOWLEDGMENT

The author wishes to thank Lynn J. Torak for furnishing drafts of several of the illustrations and the draft of the section entitled "Comparisons of Numerical Results with Analytical Solutions."

FINITE-ELEMENT FORMULATION IN CARTESIAN COORDINATES

GOVERNING FLOW EQUATION AND BOUNDARY CONDITIONS

Ground-water flow in an aquifer where there are no discontinuities in transmissivity is assumed to be governed by the two-dimensional, unsteady-state flow equation (Bear, 1979, p. 103-116)

$$\frac{\partial}{\partial x}\left(T_{xx}\frac{\partial h}{\partial x} + T_{xy}\frac{\partial h}{\partial y}\right) + \frac{\partial}{\partial y}\left(T_{yx}\frac{\partial h}{\partial x} + T_{yy}\frac{\partial h}{\partial y}\right)$$

$$+ R(H-h) + W + P = S\frac{\partial h}{\partial t}, \tag{1}$$

where

(x,y) = Cartesian coordinate directions [length],

t = time [time],

$h(x,y,t)$ = hydraulic head in the aquifer [length],

$H(x,y,t)$ = hydraulic head at the distal side of a confining unit [length],

$\begin{bmatrix} T_{xx}(x,y,t) & T_{xy}(x,y,t) \\ T_{yx}(x,y,t) & T_{yy}(x,y,t) \end{bmatrix}$ = symmetric transmissivity tensor written in matrix form $\left[\text{length}^2/\text{time}\right]$,

$R(x,y,t)$ = hydraulic conductance (vertical hydraulic conductivity divided by thickness) of a confining unit [time^{-1}],

$S(x,y,t)$ = storage coefficient [0],

$W(x,y,t)$ = unit areal recharge or discharge rate [length/time] (positive for recharge), and

$P(x,y,t) = \sum_{j=1}^{p}\delta\left(x-a_j'\right)\delta\left(y-b_j'\right)Q_j(t)$ = designation using Dirac delta functions for p point sources or sinks, each of strength Q_j [length^3/time] (positive for injection) and located at $x = a_j'$ and $y = b_j'$.

Equation (1) is subject to the following boundary and initial conditions:

1. At a discontinuity in transmissivity within the aquifer, hydraulic head and the component of flow normal to the discontinuity are unchanged as the discontinuity is crossed (Bear, 1979, p. 100-102). Thus, at a discontinuity in transmissivity between transmissivity zones a and b (figure 1),

$$h\big|_a = h\big|_b \tag{2}$$

and

$$q_n\big|_a = q_n\big|_b, \tag{3}$$

where $\cdot\big|_a$ and $\cdot\big|_b$ indicate evaluation just within the a and b sides of the discontinuity, respectively, and $q_n(x,y,t)$ is the normal component of flow (specific discharge times aquifer thickness).

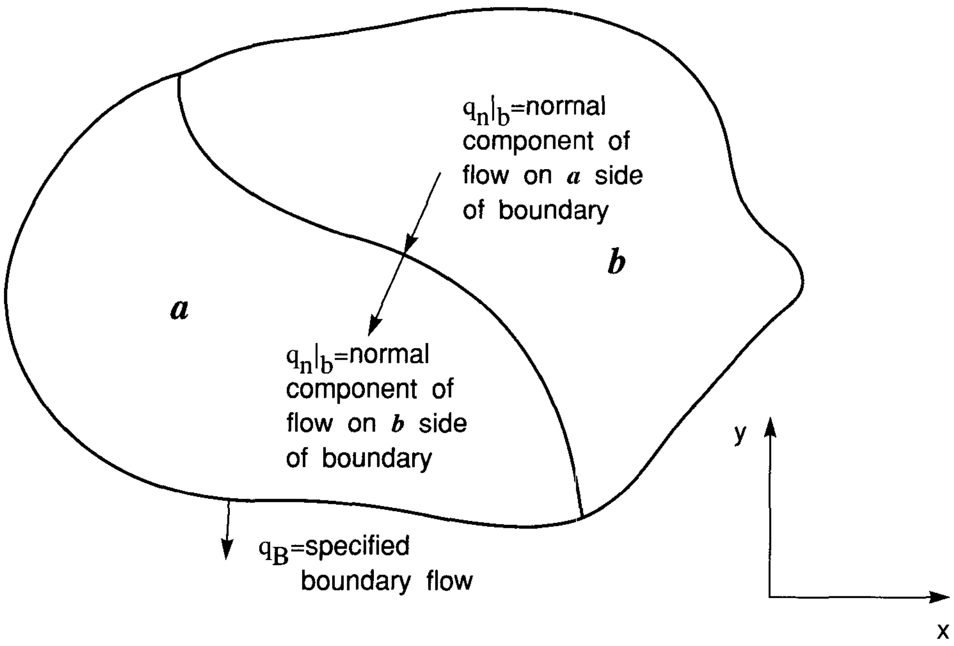

Figure 1. A hypothetical aquifer that has a discontinuity in transmissivity between zones a and b.

2. The normal component of flow across a boundary of the aquifer is given by the sum of specified and head-dependent flow components (Bear, 1979, p. 117-120). Thus, on this type of boundary

$$q_n = q_B + \alpha\left(H_B - h\right), \tag{4}$$

where

$q_B(x,y,t)$ = specified flow (specific discharge times aquifer thickness) normal to the boundary [length²/time] (positive for inflow),

$\alpha(x,y,t)$ = a parameter that approaches infinity for a specified-head (Dirichlet) condition, is zero for a specified flow (Neumann) condition, and is finite and positive for a general or mixed (Cauchy) condition [length/time], and

$H_B(x,y,t)$ = specified head at the boundary [length].

Note that although equation (4) is usually used to specify external boundary conditions (see Bear, 1979, p. 116-123, for examples), it may also be used to specify internal sources and sinks such as rivers (which are idealized as lines) or springs (which are idealized as points).

3. The hydraulic head is known everywhere at the initial instant of time, or

$$h = H_o, \tag{5}$$

where

$H_o(x,y)$ = the initial head [length].

For convenience in subsequent discussions, specified flow ($\alpha = 0$ in equation (4)) and Cauchy ($0 < \alpha < \infty$ in equation 4)) boundary conditions are referred to as Cauchy-type boundary conditions, because the former is simply a special case of the latter. Specified-head boundary conditions are treated separately from Cauchy-type boundary conditions.

FINITE-ELEMENT DISCRETIZATION

The finite-element method is used to solve equations (1) through (5). The basic concept underlying the finite-element method is that a complex flow region or domain may be subdivided into a network of subregions or elements, each having a simple shape (figure 2a). Each of these elements is then assumed to be small enough that at any instant of time the true solution, h, of equations (1) through (5) may be approximated within the element by a simple function, $\hat{h}$. These local functions are continuous across element boundaries to ensure that the approximate solution is spatially continuous. Presumably, as each element is reduced in size and the number of elements is increased, the approximate solution approaches the true solution.

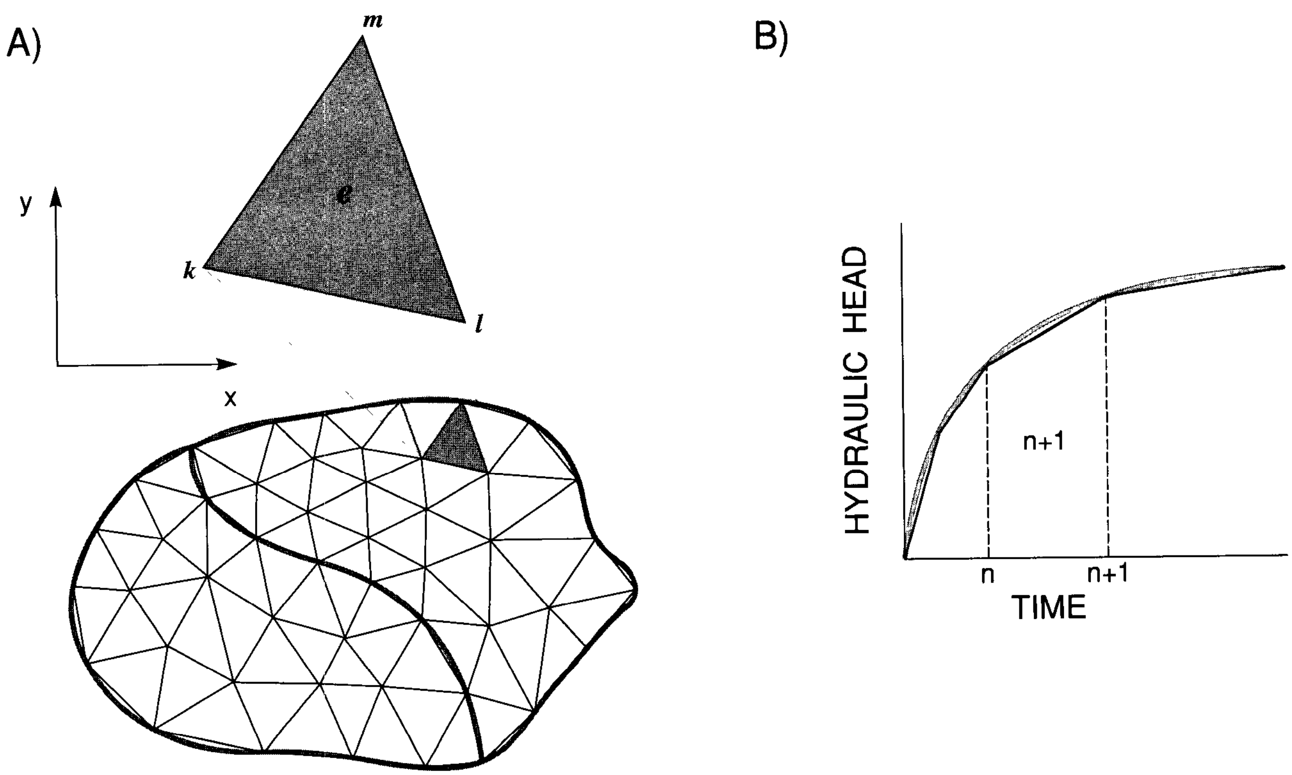

Figure 2. (a) Hypothetical aquifer of figure 1 subdivided into spatial finite elements, and (b) variation of hydraulic head with time subdivided into time elements.

The time domain of the true solution is similarly subdivided into elements (figure 2b), each bounded by two points in time at which local approximate functions are linked to form a piecewise continuous function of time. First the spatial functions are developed, then the time functions are superimposed.

In the present report, spatial element shapes are assumed to be triangles (figure 2a) and head, $\hat{h}$, is assumed to vary linearly within each element. Element corners are called nodes. Because three points define a plane, the three nodes of each triangular element are used to define the linear function.

At any point within typical element e (figure 2a) having nodes k, l, and m, the approximate solution may be written as

$$\hat{h} = A^e + B^e x + C^e y, \tag{6}$$

where constants A^e, B^e, and C^e can be found from the simultaneous equations that must be satisfied at the nodes:

$$\begin{aligned}
\hat{h}_k &= A^e + B^e x_k + C^e y_k,\\
\hat{h}_l &= A^e + B^e x_l + C^e y_l,\\
\hat{h}_m &= A^e + B^e x_m + C^e y_m,
\end{aligned} \tag{7}$$

Solution of equations (7) for A^e, B^e, and C^e, substitution of the results into equation (6), and rearrangement yields the final equation (Segerlind, 1976, p. 28-30)

$$\hat{h} = \hat{h}_k N_k^e + \hat{h}_l N_l^e + \hat{h}_m N_m^e, \tag{8}$$

where

$$\begin{aligned}
\hat{h}_i &= \hat{h}\left(x_i, y_i, t\right), \quad i = k,l,m,\\
N_i^e &= \left(a_i^e + b_i^e x + c_i^e y\right)/2\Delta^e, \quad i = k,l,m,
\end{aligned} \tag{9}$$

and the N_i^e are called basis (or coordinate) functions. In equations (9),

$$\begin{aligned}
a_k^e &= x_l y_m - x_m y_l,\\
b_k^e &= y_l - y_m,\\
c_k^e &= x_m - x_l,\\
a_l^e &= x_m y_k - x_k y_m,\\
b_l^e &= y_m - y_k,\\
c_l^e &= x_k - x_m,\\
a_m^e &= x_k y_l - x_l y_k,\\
b_m^e &= y_k - y_l,\\
c_m^e &= x_l - x_k,
\end{aligned} \tag{10}$$

and

$$2\Delta^e = \left(x_k - x_m\right)\left(y_l - y_m\right) - \left(x_m - x_l\right)\left(y_m - y_k\right). \tag{11}$$

If nodes k, l, and m are numbered counter-clockwise around element e, then Δ^e is the area of element e. Otherwise, Δ^e is the negative of the area. Following the counter-clockwise numbering convention is critical to maintain the proper signs of quantities in the finite-element equations to be developed.

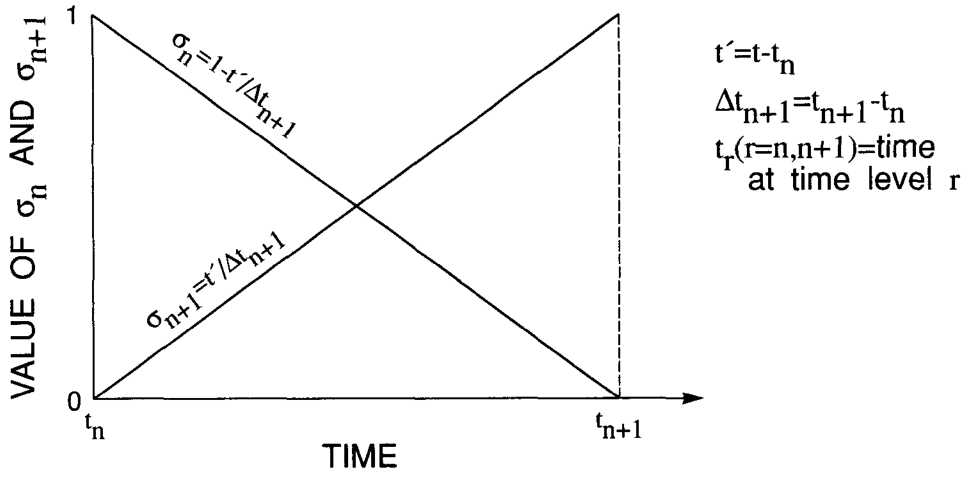

Figure 3. Finite-element discretization of time using basis functions σ_n and σ_{n+1} (after Zienkiewicz, 1971, p. 337).

Useful properties of the N_i^e are given by Wang and Anderson (1982, p. 120) as:

1. N_i^e is 1 at node i and 0 at the other two nodes.

2. N_i^e varies linearly with distance along any side.

3. N_i^e is 0 along the side opposite node i.

4. N_i^e is 1/3 at the centroid of the triangular element.

Another easily verified, useful property is that $N_k^e + N_l^e + N_m^e = 1$ at any point (x,y) in element e.

An approximate solution over time is developed by using the same finite-element concepts used to derive the approximate solution in space (Zienkiewicz, 1971, p. 335-337). Finite elements in time are chosen to be one-dimensional, and basis functions σ are chosen to be linear with a time node at each end of each element (figure 2b). If times at two time nodes are designated as t_n and t_{n+1}, and the length $t_{n+1} - t_n$ of a time element is Δt_{n+1} (figure 3), then hydraulic head $\hat{h}$ can be written for each space node i within each time element as

$$\hat{h}_i = \hat{h}_{i,n}\, \sigma_n + \hat{h}_{i,n+1}\, \sigma_{n+1}, \tag{12}$$

where the basis functions are given by

$$\sigma_n = 1 - \frac{t'}{\Delta t_{n+1}}, \qquad \sigma_{n+1} = \frac{t'}{\Delta t_{n+1}}, \tag{13}$$

$t' = t - t_n$, and $\hat{h}_{i,r} = \hat{h}_i\left(t_r\right)$, r = n, n + 1. The basis functions σ_n and σ_{n+1} satisfy the first three properties listed for N_i^e previously, modified accordingly for the one-dimensional nature of the time element.

Combination of equations (8) and (12) yields the final approximate solution

$$\hat{h} = \sum_i \left(\hat{h}_{i,n}\, \sigma_n + \hat{h}_{i,n+1}\, \sigma_{n+1} \right) N_i^e, \quad i = k,l,m. \tag{14}$$

Nodal hydraulic heads in equation (14) are calculated so that $\hat{h}$ approximates the true solution, as described in the following section.

DERIVATION OF FINITE-ELEMENT EQUATIONS

Assume that there are N nodes in the flow domain, and that we wish to solve for values of hydraulic head at all N nodes. The necessary equations are generated by the approximate solution of equations (1) through (5), which is commonly derived using either weighted residual methods (Zienkiewicz, 1971, chap. 3; Norrie and deVries, 1973, chaps. 2 and 5; Pinder and Gray, 1977, chap. 3) or classical variational methods (Zienkiewicz, 1971, chaps. 3, 15, and 16; Remson and others, 1971, chap. 7; Norrie and deVries, 1973, chaps. 3-6, 9, 10). In weighted residual methods, solution over space is generally carried out separately from solution over time. To derive the necessary equations, the approximate solution given by equation (8) is substituted into equation (1) to form a residual, which is then multiplied by each member of a set of N weighting functions and integrated over the flow domain. The resulting set of N equations is then manipulated using the boundary conditions (equations (2) and (4)) to yield a set of N ordinary differential equations in time, which are usually solved with finite-difference methods. A commonly used weighted residual method is the Galerkin method, where the weighting functions are the basis functions N_i, each of which is the union of all elemental basis functions N_i^e. A Galerkin in time method was given by Zienkiewicz (1971, p. 335-336) as an alternative to the finite-difference solution over time.

The classical variational method involves use of a variational principle, which is an integral that, when minimized over the flow domain, yields equations (1) and (4). Because this variational principal is equivalent to the flow problem, the approximate solution may be substituted into it, and the integral may be minimized with respect to each nodal value of hydraulic head to yield the required finite-element equations. Variational and Galerkin finite-element methods applied to equations (1) through (5) yield the same set of finite-element equations when the same approximate solution (for example, equation (8)) is used.

Error-functional justification for the finite-element equations

Another method that is closely related to the classical variational method is to fit the approximate solution to the true solution using an integral functional[1] of the error, $\hat{e} = h-\hat{h}$. In this author's opinion, derivation of the finite-element equations with this method is easier and provides more direct insight into the nature of the solution in terms of its error than the other methods.

[1]A functional is a function of a function. The integral is a function of the error $\hat{e} = h-\hat{h}$, and $\hat{e}$ is regarded as a function of the values of $\hat{h}_{i,n+1}$; hence, the integral is a functional.

To be useful, the functional, termed $I(\hat{e})$, must be defined such that (1) $I(\hat{e}) \geq 0$, with equality occurring only if $\hat{e} = 0$, (2) the true solution, h, can be eliminated from the final finite-element equations, and (3) $I(\hat{e})$ measures total (or integrated) error over the entire flow domain. The only error functional that satisfies these requirements and produces the same equations as produced by the Galerkin and classical variational methods is

$$I(\hat{e}) = \sum_{e} \int_{0}^{\Delta t_{n+1}} \left\{ \iint_{\Delta^e} \left[\frac{\partial \hat{e}}{\partial x}\left(T_{xx} \frac{\partial \hat{e}}{\partial x} + T_{xy} \frac{\partial \hat{e}}{\partial y}\right) + \frac{\partial \hat{e}}{\partial y}\left(T_{yx} \frac{\partial \hat{e}}{\partial x} + T_{yy} \frac{\partial \hat{e}}{\partial y}\right) + R\hat{e}^2 + S\left(\frac{\partial \hat{e}}{\partial t}\right)^2 t' \right] dxdy + \int_{C_2^e} \alpha \hat{e}^2 \, dC \right\} dt', \tag{15}$$

where the sum over e indicates the sum over all elements, the double integral over Δ^e indicates integration over spatial element e, and the contour integral over C_2^e indicates integration over the side (if any) of element e that is part of a boundary where a Cauchy-type boundary condition applies. For equation (15) to be valid, the matrix of transmissivities must be symmetric and positive definite, and R, S, and α must be greater than or equal to zero. The requirement for the transmissivities guarantees that the sum of terms involving transmissivities is positive (or zero if $\hat{e} = 0$) because this sum is a positive-definite quadratic form (see Hohn, 1964, p. 336, 338). Note that for ground-water flow problems, all of these requirements are satisfied.

The approximate solution is fitted to the true solution by minimizing $I(\hat{e})$ with respect to the approximate solution, which leads to an error distribution in which the error at any point (x,y,t) is as small as possible as measured by $I(\hat{e})$. Because functional $I(\hat{e})$ includes terms involving the error and its spatial and temporal derivatives, the minimization process minimizes the combination of the error and its derivatives. Magnitudes of T_{xx} (etc.), R, S, and α indicate which types of terms are more heavily weighted, and thus have more influence on the solution, for any given problem. For example, if terms involving the error directly were heavily weighted (that is, R and (or) α were large) compared to the other terms, then the average (integrated) error should be small, but if terms involving derivatives were heavily weighted, then the average error might be large if large errors were required to make the average derivatives of the error small. This latter situation could arise if space or time elements were too large or were poorly configured.

Minimization of equation (15) is accomplished by taking its derivative with respect to each value of $\hat{h}_{i,n+1}$, $i = 1,2,\cdots,N$, and setting each result to zero. Equation (15) does not also have to be minimized with respect to

$\hat{h}_{i,n}$ because an equation for time level n was created by minimizing equation (15) with respect to $\hat{h}_{i,n+1}$ for the previous time element. For the initial time element, $\hat{h}_{i,0}$ is the known initial condition so that equation (15) is not minimized with respect to it. It can be readily verified that the result of minimization is

$$\frac{\partial I}{\partial \hat{h}_{i,n+1}} = -2\sum_{e_i} \int_0^{\Delta t_{n+1}} \sigma_{n+1} \left\{ \iint_{\Delta^e} \left[\frac{\partial N_i^e}{\partial x}\left(T_{xx}\frac{\partial \hat{e}}{\partial x} + T_{xy}\frac{\partial \hat{e}}{\partial y}\right) + \frac{\partial N_i^e}{\partial y}\left(T_{yx}\frac{\partial \hat{e}}{\partial x} + T_{yy}\frac{\partial \hat{e}}{\partial y}\right) + N_i^e R\hat{e} + N_i^e S\frac{\partial \hat{e}}{\partial t}\right] dxdy + \int_{C_2^e} N_i^e \alpha \hat{e} dC \right\} dt' = 0,\ i = 1,2,\cdots,N, \tag{16}$$

where summation over e_i indicates summation over all elements sharing node i, termed a patch of elements by Wang and Anderson (1982, p. 12) (figure 4). Terms for all other elements over the flow domain drop out because $\hat{h}_{i,n+1}$ does not appear in the approximate solutions in these elements.

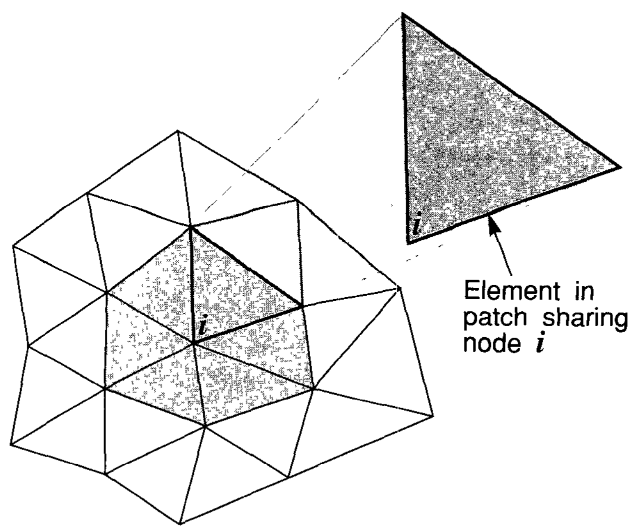

Figure 4. A typical patch of elements sharing node i.

Equation (16) can be separated into two parts, one written in terms of approximate solution $\hat{h}$ and the other written in terms of the true solution h. Thus,

$$\sum_{e_i} \int_0^{\Delta t_{n+1}\sigma_{n+1}} \left\{ \iint_{\Delta^e} \left[N_i^e \left(S\frac{\partial \hat{h}}{\partial t} - R\left(H-\hat{h}\right) - W - P \right) + \frac{\partial N_i^e}{\partial x} \left(T_{xx} \frac{\partial \hat{h}}{\partial x} + T_{xy} \frac{\partial \hat{h}}{\partial y} \right) \right. \right.$$

$$\left. \left. + \frac{\partial N_i^e}{\partial y} \left(T_{yx} \frac{\partial \hat{h}}{\partial x} + T_{yy} \frac{\partial \hat{h}}{\partial y} \right) \right] dxdy - \int_{C_2^e} N_i^e \left[q_B + \alpha\left(H_B - \hat{h}\right) \right] dC \right\} dt'$$

$$- \sum_{e_i} \int_0^{\Delta t_{n+1}\sigma_{n+1}} \left\{ \iint_{\Delta^e} \left[N_i^e \left(S\frac{\partial h}{\partial t} - R(H-h) - W - P \right) + \frac{\partial N_i^e}{\partial x} \left(T_{xx} \frac{\partial h}{\partial x} + T_{xy} \frac{\partial h}{\partial y} \right) \right. \right.$$

$$\left. \left. + \frac{\partial N_i^e}{\partial y} \left(T_{yx} \frac{\partial h}{\partial x} + T_{yy} \frac{\partial h}{\partial y} \right) \right] dxdy - \int_{C_2^e} N_i^e \left[q_B + \alpha\left(H_B - h\right) \right] dC \right\} dt' = 0. \qquad (17)$$

Note that, to make each part of equation (17) complete, several terms were added to one part of the equation and subtracted from the other part. In appendix A the sum of the terms involving the true solution is shown to equal zero, so that equation (17) becomes

$$\sum_{e_i} \int_0^{\Delta t_{n+1}\sigma_{n+1}} \left\{ \iint_{\Delta^e} \left[N_i^e \left(S\frac{\partial \hat{h}}{\partial t} - R\left(H-\hat{h}\right) - W - P \right) + \frac{\partial N_i^e}{\partial x} \left(T_{xx} \frac{\partial \hat{h}}{\partial x} + T_{xy} \frac{\partial \hat{h}}{\partial y} \right) \right. \right.$$

$$\left. \left. + \frac{\partial N_i^e}{\partial y} \left(T_{yx} \frac{\partial \hat{h}}{\partial x} + T_{yy} \frac{\partial \hat{h}}{\partial y} \right) \right] dxdy - \int_{C_2^e} N_i^e \left[q_B + \alpha\left(H_B - \hat{h}\right) \right] dC \right\} dt' = 0, \quad i = 1,2,\cdots,N. \qquad (18)$$

Equation (18) represents the required set of finite-element equations. Performing the indicated integrations yields the final set of operational equations. However, before the integrations can be accomplished, the specific space and time dependencies of the various terms in the integrals must be specified, and two desirable simplifications are made.

Integral approximations

The first simplification involves the integrals of $S\partial\hat{h}/\partial t$, $R(H-\hat{h})$, and $\alpha(H_B-\hat{h})$. These integrals do not involve spatial derivatives of $\hat{h}$ and can be shown to contribute positive terms to the diagonal and off-diagonal elements of the final coefficient matrix for the approximate solution (Segerlind, 1976, p. 216). In contrast, the integrals involving spatial derivatives contribute nonpositive off-diagonal terms and positive diagonal terms such that the sum of absolute values of the off-diagonal terms equals the diagonal term if all internal angles of the triangular elements are less than or equal to 90° (Narasimhan and others, 1978, p. 866). When specified-head boundary conditions are introduced, the coefficient matrix resulting from the spatial derivative terms is a type of M-matrix known as a Stieltjes matrix (Varga, 1962, p. 85), which is ideal for the iterative matrix solution technique introduced further on. In addition, a Stieltjes final coefficient matrix can be shown to guarantee a nonoscillatory solution to equation (18) when combined with proper restrictions in time-element size (Briggs and Dixon, 1968). Addition of positive off-diagonal terms to the matrix can destroy the Stieltjes matrix property, so that it is desirable to replace the integrals of $S\partial\hat{h}/\partial t$, $R(H-\hat{h})$, and $\alpha(H_B-\hat{h})$ with integrals that contribute only positive diagonal terms. This replacement also simplifies the resulting finite-element equations so that their solution requires less computer time and storage than if the matrices resulting from the original integrals were used.

In structural dynamics problems, replacement of the so-called consistent mass matrix (the matrix resulting from an integral involving second derivatives of time that is analogous to the integral of $S\partial\hat{h}/\partial t$) with a diagonal approximation of the mass matrix has been reported to yield degraded results (Zienkiewicz, 1971, p. 326). Similar degraded solutions were reported when a diagonal approximation was used for advection-dominated advection-diffusion problems (Gresho and others, 1976). However, Narasimhan and others (1978, p. 863-864) argue that a diagonal approximation enhances the numerical performance when applied to the integral of $S\partial\hat{h}/\partial t$, and that retaining the nondiagonal form can lead to numerical difficulties. In addition, Wilson and others (1979) obtained good correspondence between analytical and finite-element solutions of equation (1) for several different test problems by using the same diagonal approximation, linear basis functions, and triangular spatial elements as used here. The author is aware of no study indicating degraded solutions when the diagonal approximation is applied to equations (1) through (5) using triangular spatial elements and linear basis functions, and the author's own numerical experiments have not revealed any significant degradation either. Finally, the author's analysis indicates that the method used here yields consistent mass balance over each patch of elements.

The method can be demonstrated for one integral, and results for the other two are similar. The diagonal approximation is

$$\iint_{\Delta^e} SN_i^e \frac{\partial\hat{h}}{\partial t}\,dxdy \simeq \iint_{\Delta^e} SN_i^e \frac{d\hat{h}_i}{dt}\,dxdy. \qquad (19)$$

The quadratic function $N_i^e\partial\hat{h}/\partial t$ is replaced by the linear function $N_i^e d\hat{h}_i/dt$, which, for constant S over the element (which is adopted for the present report), makes the approximation equivalent to the second-order correct trapezoidal rule (McCracken and Dorn, 1964, p. 161-166).

Rotation of coordinate axes

The second simplification, which is not an approximation, involves rotating the x and y coordinate axes locally, within each element, to axes $\bar{x}$ and $\bar{y}$ that coincide with the principal directions of the transmissivity tensor (figure 5) (Zienkiewicz and others, 1966). In the rotated coordinate

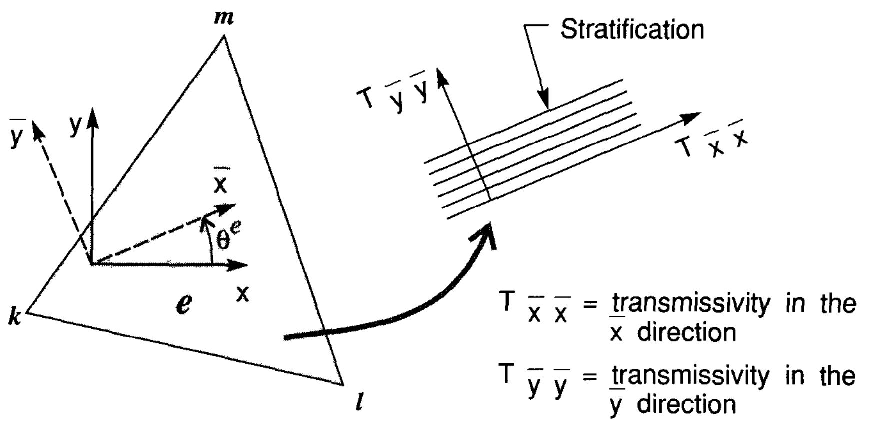

Figure 5. Rotation from global (x,y) to local ($\bar{x}$,$\bar{y}$) coordinates in element e having node numbers k, l, and m.

system, the only nonzero components of the local transmissivity tensor are the diagonal (principal) components, $T_{\bar{x}\bar{x}}$ and $T_{\bar{y}\bar{y}}$. Coordinates $\bar{x}$ and $\bar{y}$ are obtained by using the rotation equations

$$\begin{aligned} \bar{x} &= x \cos \theta^e + y \sin \theta^e, \\ \bar{y} &= -x \sin \theta^e + y \cos \theta^e, \end{aligned} \tag{20}$$

where θ^e is the angle of rotation of the axes, measured counter-clockwise, in element e (see figure 5). By replacing coordinates x and y and the original transmissivity tensor with rotated coordinates $\bar{x}$ and $\bar{y}$ and the diagonal transmissivity tensor, equation (18) can be transformed to become

$$\begin{aligned} \sum_{e_i} \int_0^{\Delta t_{n+1}} \sigma_{n+1} \Bigg\{ \iint_{\Delta^e} \Bigg[\bar{N}_i^e \left(S \frac{d\hat{h}_i}{dt} - R\left(H_i - \hat{h}_i\right) - W - P \right) + \frac{\partial \bar{N}_i^e}{\partial \bar{x}} T_{\bar{x}\bar{x}} \frac{\partial \hat{h}}{\partial \bar{x}} \\ + \frac{\partial \bar{N}_i^e}{\partial \bar{y}} T_{\bar{y}\bar{y}} \frac{\partial \hat{h}}{\partial \bar{y}} \Bigg] d\bar{x}d\bar{y} - \int_{C_2^e} \bar{N}_i^e \left[q_B + \alpha\left(H_{Bi} - \hat{h}_i\right)\right] d\bar{C} \Bigg\} dt' = 0, \quad i = 1,2,\cdots,N, \end{aligned} \tag{21}$$

where the bars over the variables indicate evaluation using $\bar{x}$ and $\bar{y}$ and equations like equation (19) were used to modify the appropriate integrals.

Evaluation of spatial integrals

To reduce notational complexity, the space and time integrations in equation (21) are performed in two separate steps. To perform the space integrations, it is assumed that S, R, and W are constant in each spatial element, and that $T_{\bar{x}\bar{x}}$ and $T_{\bar{y}\bar{y}}$ are linearly variable in each element as given by relationships analogous to equation (8). That is,

$$T_{\bar{x}\bar{x}} = T_{\bar{x}\bar{x}k}^e \bar{N}_k^e + T_{\bar{x}\bar{x}l}^e \bar{N}_l^e + T_{\bar{x}\bar{x}m}^e \bar{N}_m^e, \tag{22}$$

and

$$T_{\bar{y}\bar{y}} = T_{\bar{y}\bar{y}k}^e \bar{N}_k^e + T_{\bar{y}\bar{y}l}^e \bar{N}_l^e + T_{\bar{y}\bar{y}m}^e \bar{N}_m^e, \tag{23}$$

where $T^e_{\bar{x}\bar{x}k}$, etc., are values of transmissivity at nodes k, etc., in element e. It is further assumed that q_B and α are constant along any Cauchy-type boundary side of each element. The integration is performed for typical element e bounded by nodes k, l, and m using the general formulas (Segerlind, 1976, p. 45)

$$\iint_{\Delta^e} \left(\bar{N}^e_k\right)^p \left(\bar{N}^e_l\right)^q \left(\bar{N}^e_m\right)^r d\bar{x}d\bar{y} = \frac{p!q!r!}{(p+q+r+2)!} 2\Delta^e \tag{24}$$

and

$$\int_{L_{kl}} \left(\bar{N}^e_k\right)^p \left(\bar{N}^e_l\right)^q d\bar{C} = \frac{p!q!}{(p+q+1)!} L_{kl}, \tag{25}$$

where L_{kl} is the length of the element side between nodes k and l. Thus, by writing $\hat{h}$ using equation (8) and substituting the appropriate expressions for $\bar{N}^e_i$, $\partial\bar{N}^e_i/\partial\bar{x}$, and $\partial\bar{N}^e_i/\partial\bar{y}$, i = k,l,m, the spatial integrals in equation (21) are evaluated for i = k (for example) as

$$\iint_{\Delta^e} \bar{N}^e_k S \frac{d\hat{h}_k}{dt} d\bar{x}d\bar{y} = \frac{1}{3}S^e\Delta^e \frac{d\hat{h}_k}{dt}, \tag{26}$$

$$\iint_{\Delta^e} \bar{N}^e_k R\left(H_k-\hat{h}_k\right) d\bar{x}d\bar{y} = \frac{1}{3}R^e\Delta^e\left(H_k-\hat{h}_k\right), \tag{27}$$

$$\iint_{\Delta^e} \bar{N}^e_k W d\bar{x}d\bar{y} = \frac{1}{3}W^e\Delta^e, \tag{28}$$

$$\iint_{\Delta^e} \bar{N}^e_k P d\bar{x}d\bar{y} = \iint_{\Delta^e} \bar{N}^e_k \sum_{j=1}^{P_e} \delta\left(\bar{x}-\bar{a}'_j\right) \delta\left(\bar{y}-\bar{b}'_j\right) Q_j d\bar{x}d\bar{y}$$

$$= \sum_{j=1}^{P_e} \bar{N}^e_k\left(\bar{a}'_j,\bar{b}'_j\right)Q_j = P^e_k, \tag{29}$$

$$\iint_{\Delta^e} \frac{\partial\bar{N}^e_k}{\partial\bar{x}} T_{\bar{x}\bar{x}} \frac{\partial\hat{h}}{\partial\bar{x}} d\bar{x}d\bar{y} = \iint_{\Delta^e} \frac{\partial\bar{N}^e_k}{\partial\bar{x}}\left(T^e_{\bar{x}\bar{x}k} \bar{N}^e_k + T^e_{\bar{x}\bar{x}l} \bar{N}^e_l + T^e_{\bar{x}\bar{x}m} \bar{N}^e_m\right)\cdot$$

$$\cdot \left(\frac{\partial \bar{N}_k^e}{\partial \bar{x}} \hat{h}_k + \frac{\partial \bar{N}_1^e}{\partial \bar{x}} \hat{h}_1 + \frac{\partial \bar{N}_m^e}{\partial \bar{x}} \hat{h}_m \right) d\bar{x}d\bar{y}$$

$$= \frac{T^e_{\bar{x}\bar{x}}}{4\Delta^e} \left(\bar{b}_k^e \bar{b}_k^e \hat{h}_k + \bar{b}_k^e \bar{b}_1^e \hat{h}_1 + \bar{b}_k^e \bar{b}_m^e \hat{h}_m \right), \tag{30}$$

$$\int_{\Delta^e}\int \frac{\partial \bar{N}_k^e}{\partial \bar{y}} T_{\bar{y}\bar{y}} \frac{\partial \hat{h}}{\partial \bar{y}} d\bar{x}d\bar{y} = \int_{\Delta^e}\int \frac{\partial \bar{N}_k^e}{\partial \bar{y}} \left(T^e_{\bar{y}\bar{y}k} \bar{N}_k^e + T^e_{\bar{y}\bar{y}1} \bar{N}_1^e + T^e_{\bar{y}\bar{y}m} \bar{N}_m^e \right) \cdot$$

$$\cdot \left(\frac{\partial \bar{N}_k^e}{\partial \bar{y}} \hat{h}_k + \frac{\partial \bar{N}_1^e}{\partial \bar{y}} \hat{h}_1 + \frac{\partial \bar{N}_m^e}{\partial \bar{y}} \hat{h}_m \right) d\bar{x}d\bar{y}$$

$$= \frac{T^e_{\bar{y}\bar{y}}}{4\Delta^e} \left(\bar{c}_k^e \bar{c}_k^e \hat{h}_k + \bar{c}_k^e \bar{c}_1^e \hat{h}_1 + \bar{c}_k^e \bar{c}_m^e \hat{h}_m \right), \tag{31}$$

$$\int_{C_2^e} \bar{N}_k^e \left[q_B + \alpha \left(H_{Bk} - \hat{h}_k \right) \right] d\bar{C} = \frac{1}{2} \left[\left(q_B L \right)_{k1} + \left(\alpha L \right)_{k1} \left(H_{Bk} - \hat{h}_k \right) \right.$$

$$\left. + \left(q_B L \right)_{km} + \left(\alpha L \right)_{km} \left(H_{Bk} - \hat{h}_k \right) \right], \tag{32}$$

where S^e, R^e, and W^e are the constant values of S, R, and W in element e;

$$T^e_{\bar{x}\bar{x}} = \frac{1}{3} \left(T^e_{\bar{x}\bar{x}k} + T^e_{\bar{x}\bar{x}1} + T^e_{\bar{x}\bar{x}m} \right); \tag{33}$$

$$T^e_{\bar{y}\bar{y}} = \frac{1}{3} \left(T^e_{\bar{y}\bar{y}k} + T^e_{\bar{y}\bar{y}1} + T^e_{\bar{y}\bar{y}m} \right); \tag{34}$$

$\bar{b}_i^e$ and $\bar{c}_i^e$, i = k,l,m, are defined by equations (10) and evaluated using $\bar{x}$ and $\bar{y}$; p_e is the number of point sources and sinks in element e; $\bar{N}_k^e\left(\bar{a}_j',\bar{b}_j'\right)$ is the basis function for node k evaluated at point $\left(\bar{a}_j',\bar{b}_j'\right)$; and L_{k1} and L_{km} are lengths of element sides between nodes k and 1 and between nodes k and m, respectively, on a Cauchy-type boundary. If a side is not on a Cauchy-type boundary, then L for that side is set to zero.

The term P_k^e represents the total amount of pumping that is allocated to node k in element e. If a well is located at node k (where $\bar{a}_j' = \bar{x}_k$ and $\bar{b}_j' = \bar{y}_k$ so that $\bar{N}_k^e\left(\bar{a}_j',\bar{b}_j'\right) = 1$), then the pumping rate Q_j can be allocated to one element so that when summed over all elements in the patch, the total rate is still Q_j. For other points in element e, the rate allocated to node k is less than the total rate Q_j because $\bar{N}_k^e\left(\bar{a}_j',\bar{b}_j'\right) < 1$ for $\bar{a}_j' \neq \bar{x}_k$ and (or) $\bar{b}_j' \neq \bar{y}_k$. However, parts of Q_j are also allocated to the other two nodes of the element so that, because $\bar{N}_k^e + \bar{N}_l^e + \bar{N}_m^e = 1$, the sum of the rates allocated to the three nodes is Q_j, as required.

By using equations (26) through (34), the spatial integrals for element e in equation (21) can be written as

$$\iint_{\Delta^e} \left[\bar{N}_k^e\left(S\frac{d\hat{h}_k}{dt} - R\left(H_k-\hat{h}_k\right) - W - P\right) + \frac{\partial \bar{N}_k^e}{\partial \bar{x}} T_{\bar{x}\bar{x}} \frac{\partial \hat{h}}{\partial \bar{x}} + \frac{\partial \bar{N}_k^e}{\partial \bar{y}} T_{\bar{y}\bar{y}} \frac{\partial \hat{h}}{\partial \bar{y}}\right] d\bar{x}d\bar{y}$$

$$-\int_{C_2^e} \bar{N}_k^e\left[q_B + \alpha\left(H_{Bk}-\hat{h}_k\right)\right] d\bar{C}$$

$$= c_{kk}^e \frac{d\hat{h}_k}{dt} + \left(g_{kk}^e + v_{kk}^e\right)\hat{h}_k + g_{kl}^e\hat{h}_l + g_{km}^e\hat{h}_m - \frac{1}{3}R^e\Delta^e H_k - \frac{1}{3}W^e\Delta^e - P_k^e$$

$$-\frac{1}{2}\left[\left(q_BL\right)_{kl} + \left(q_BL\right)_{km}\right] - \frac{1}{2}\left[\left(\alpha L\right)_{kl} + \left(\alpha L\right)_{km}\right]H_{Bk}, \tag{35}$$

where

$$c_{kk}^e = \frac{1}{3}S^e\Delta^e, \tag{36}$$

$$v_{kk}^e = \frac{1}{3}R^e\Delta^e + \frac{1}{2}\left[\left(\alpha L\right)_{kl} + \left(\alpha L\right)_{km}\right], \tag{37}$$

$$g_{kk}^e = \frac{T_{\bar{x}\bar{x}}^e}{4\Delta^e}\,\bar{b}_k^e\bar{b}_k^e + \frac{T_{\bar{y}\bar{y}}^e}{4\Delta^e}\,\bar{c}_k^e\bar{c}_k^e, \tag{38}$$

$$g_{kl}^{e} = \frac{T_{\bar{x}\bar{x}}^{e}}{4\Delta^{e}} \bar{b}_k^e \bar{b}_l^e + \frac{T_{\bar{y}\bar{y}}^{e}}{4\Delta^{e}} \bar{c}_k^e \bar{c}_l^e, \tag{39}$$

$$g_{km}^{e} = \frac{T_{\bar{x}\bar{x}}^{e}}{4\Delta^{e}} \bar{b}_k^e \bar{b}_m^e + \frac{T_{\bar{y}\bar{y}}^{e}}{4\Delta^{e}} \bar{c}_k^e \bar{c}_m^e. \tag{40}$$

A small alteration in the integral formulations given by equations (30) and (31) is useful for computations and in developments further on. Because $\bar{N}_k^e + \bar{N}_l^e + \bar{N}_m^e = 1$, the terms

$$-\left(\frac{\partial \bar{N}_k^e}{\partial \bar{x}} + \frac{\partial \bar{N}_l^e}{\partial \bar{x}} + \frac{\partial \bar{N}_m^e}{\partial \bar{x}}\right)\hat{h}_k$$

and

$$-\left(\frac{\partial \bar{N}_k^e}{\partial \bar{y}} + \frac{\partial \bar{N}_l^e}{\partial \bar{y}} + \frac{\partial \bar{N}_m^e}{\partial \bar{y}}\right)\hat{h}_k$$

are both equal to zero and can be added into the terms

$$\frac{\partial \bar{N}_k^e}{\partial \bar{x}} \hat{h}_k + \frac{\partial \bar{N}_l^e}{\partial \bar{x}} \hat{h}_l + \frac{\partial \bar{N}_m^e}{\partial \bar{x}} \hat{h}_m$$

and

$$\frac{\partial \bar{N}_k^e}{\partial \bar{y}} \hat{h}_k + \frac{\partial \bar{N}_l^e}{\partial \bar{y}} \hat{h}_l + \frac{\partial \bar{N}_m^e}{\partial \bar{y}} \hat{h}_m$$

in equations (30) and (31), respectively. The resulting modifications of equations (30) and (31) are

$$\iint_{\Delta^e} \frac{\partial \bar{N}_k^e}{\partial \bar{x}} T_{\bar{x}\bar{x}} \frac{\partial \hat{h}}{\partial \bar{x}} d\bar{x}d\bar{y} = \frac{T_{\bar{x}\bar{x}}^{e}}{4\Delta^{e}}\left[\bar{b}_k^e \bar{b}_l^e\left(\hat{h}_l - \hat{h}_k\right) + \bar{b}_k^e \bar{b}_m^e\left(\hat{h}_m - \hat{h}_k\right)\right] \tag{41}$$

and

$$\iint_{\Delta^e} \frac{\partial \bar{N}_k^e}{\partial \bar{y}} T_{\bar{y}\bar{y}} \frac{\partial \hat{h}}{\partial \bar{y}} d\bar{x}d\bar{y} = \frac{T_{\bar{y}\bar{y}}^{e}}{4\Delta^{e}}\left[\bar{c}_k^e \bar{c}_l^e\left(\hat{h}_l - \hat{h}_k\right) + \bar{c}_k^e \bar{c}_m^e\left(\hat{h}_m - \hat{h}_k\right)\right], \tag{42}$$

which indicates that

$$g_{kk}^{e} = -g_{kl}^{e} - g_{km}^{e}. \tag{43}$$

The revised formulation, which was used by Narasimhan and others (1978, p. 875), saves both computer time and storage requirements because g_{kk}^{e} never need be explicitly computed using equation (38). An added advantage over the original formulation is that equations (41) and 42) generate less round-off error than equations (30) and (31) when solving the simultaneous systems of equations developed further on.

Substitution of equation (35) into equation (21) written for node k yields

$$\sum_{e_k}\int_0^{\Delta t_{n+1}}\sigma_{n+1}\left\{c_{kk}^e\frac{d\hat{h}_k}{dt}+\left(g_{kk}^e+v_{kk}^e\right)\hat{h}_k+g_{kl}^e\hat{h}_l+g_{km}^e\hat{h}_m-\frac{1}{3}R^e\Delta^e H_k-\frac{1}{3}W^e\Delta^e-P_k^e\right.$$
$$\left.-\frac{1}{2}\left[\left(q_BL\right)_{kl}+\left(q_BL\right)_{km}\right]-\frac{1}{2}\left[\left(\alpha L\right)_{kl}+\left(\alpha L\right)_{km}\right]H_{Bk}\right\}dt'=0. \tag{44}$$

Equation (44) must apply to all N nodes of the finite-element mesh. These N equations can be written in matrix form as

$$\int_0^{\Delta t_{n+1}}\sigma_{n+1}\left[\underline{\underline{C}}\frac{d\underline{\hat{h}}}{dt}+\left(\underline{\underline{G}}+\underline{\underline{V}}\right)\underline{\hat{h}}-\underline{B}\right]dt'=\int_0^{\Delta t_{n+1}}\sigma_{n+1}\left(\underline{\underline{C}}\frac{d\underline{\hat{h}}}{dt}+\underline{\underline{A}}\underline{\hat{h}}-\underline{B}\right)dt'=\underline{0}, \tag{45}$$

where

$$\underline{\underline{A}}=\underline{\underline{G}}+\underline{\underline{V}}, \tag{46}$$

and doubly underscored letters indicate matrices and singly underscored letters indicate vectors. Entries of the matrices and vectors are defined as follows:

$$C_{ij}=\begin{cases}\sum_{e_i} c_{ij}^e, & i=j\\ 0, & i\neq j\end{cases}, \tag{47}$$

$$V_{ij}=\begin{cases}\sum_{e_i} v_{ij}^e, & i=j\\ 0, & i\neq j\end{cases}, \tag{48}$$

$$G_{ij}=\sum_{e_i} g_{ij}^e, \tag{49}$$

$$B_i=\sum_{e_i}\left[\frac{1}{3}R^e\Delta^e H_i+\frac{1}{3}W^e\Delta^e+P_i^e+\frac{1}{2}\sum_{j'}\left(q_BL\right)_{ij'}+\frac{1}{2}\sum_{j'}(\alpha L)_{ij'}H_{Bi}\right], \tag{50}$$

where the sum over j′ indicates the sum over the two nodes that are adjacent to node i in an element.

Specified-head boundaries were not considered in the preceding development. If node k was designated as a specified-head node, then equation (44) would be replaced by

$$\int_0^{\Delta t_{n+1}}\sigma_{n+1}\left(\hat{h}_k-H_{Bk}\right)dt'=0, \tag{51}$$

and this equation would replace equation k in matrix equation (45). Note that setting h_k equal to H_{Bk} is formally equivalent to letting $\alpha \to \infty$ at node k in equation (44).

Example of equation assembly

A simple finite-element mesh shown in figure 6 is used to demonstrate how the terms of equation (45) are assembled. Matrices $\underline{\underline{C}}$ and $\underline{\underline{A}}$, and vector $\underline{B}$, are assembled separately, then these are used to obtain the final system of equations.

Assembly is based on the patch of elements concept, where contributions to any equation i (that is, row i of $\underline{\underline{C}}$, $\underline{\underline{A}}$, or $\underline{B}$) come from all elements sharing node i. By using this concept, $\underline{\underline{C}}$ can be assembled to yield: (Note: In the following equations all zero entries are left blank.)

$$
\underline{\underline{C}} = \begin{array}{c}
\\ 1 \\ 2 \\ 3 \\ 4 \\ 5
\end{array}
\begin{array}{c}
\begin{array}{ccccc} 1 & \quad 2 \quad & \quad 3 \quad & \quad 4 \quad & 5 \end{array} \\
\left[\begin{array}{ccccc}
\frac{1}{3}S^1\Delta^1 & & & & \\
 & \frac{1}{3}\left(S^1\Delta^1+S^2\Delta^2\right) & & & \\
 & & \frac{1}{3}\left(S^1\Delta^1+S^2\Delta^2+S^3\Delta^3\right) & & \\
 & & & \frac{1}{3}\left(S^2\Delta^2+S^3\Delta^3\right) & \\
 & & & & \frac{1}{3}S^3\Delta^3
\end{array}\right]
\end{array},
$$

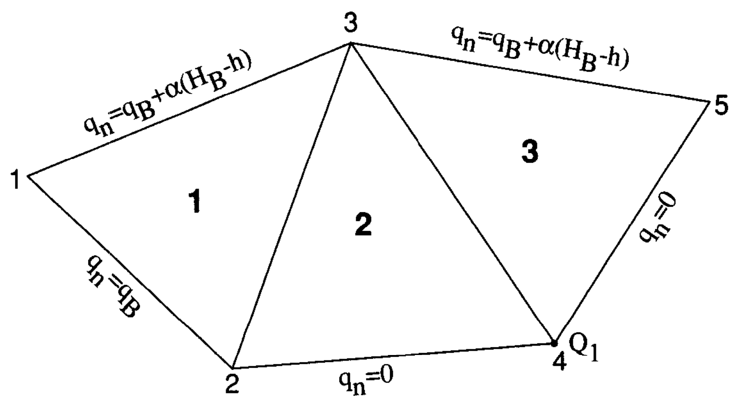

q_n = flow normal to an element boundary

q_B = specified flow normal to an element boundary

α = proportionality parameter for a Cauchy-type boundary condition

H_B = specified head at a boundary

h = hydraulic head

Q_1 = volumetric recharge from a well at node 4

Figure 6. Example of three elements and five nodes for demonstrating assembly of finite-element equations.

Matrix $\underline{\underline{A}}$ can be thought of as the sum of three matrices, a matrix composed of the g_{ij}^{e} $(i \neq j)$ terms, a matrix composed of the $\frac{1}{3}R^e\Delta^e$ terms, and a matrix composed of the $\frac{1}{2}\left(\alpha L\right)_{ij}$, terms. These matrices are defined as $\underline{\underline{G}}$, $\underline{\underline{R}}$, and $\underline{\underline{\alpha}}$, respectively, where, from equations (37) and (48), $\underline{\underline{R}} + \underline{\underline{\alpha}} = \underline{\underline{V}}$. For the mesh shown in figure 6,

$$\underline{\underline{G}} = \begin{array}{c c} & \begin{array}{ccccc} 1 & 2 & 3 & 4 & 5 \end{array} \\ \begin{array}{c} 1 \\ 2 \\ 3 \\ 4 \\ 5 \end{array} & \begin{bmatrix} -\left(g_{12}^1+g_{13}^1\right) & g_{12}^1 & g_{13}^1 & & \\ g_{21}^1 & -\left(g_{21}^1+g_{23}^1+g_{23}^2+g_{24}^2\right) & g_{23}^1+g_{23}^2 & g_{24}^2 & \\ g_{31}^1 & g_{32}^1+g_{32}^2 & -\left(g_{31}^1+g_{32}^1+g_{32}^2+g_{34}^2+g_{34}^3+g_{35}^3\right) & g_{34}^2+g_{34}^3 & g_{35}^3 \\ & g_{42}^2 & g_{43}^2+g_{43}^3 & -\left(g_{42}^2+g_{43}^2+g_{43}^3+g_{45}^3\right) & g_{45}^3 \\ & & g_{53}^3 & g_{54}^3 & -\left(g_{53}^3+g_{54}^3\right) \end{bmatrix} \end{array},$$

$$\underline{\underline{R}} = \begin{array}{c c} & \begin{array}{ccccc} 1 & 2 & 3 & 4 & 5 \end{array} \\ \begin{array}{c} 1 \\ 2 \\ 3 \\ 4 \\ 5 \end{array} & \begin{bmatrix} \frac{1}{3}R^1\Delta^1 & & & & \\ & \frac{1}{3}\left(R^1\Delta^1+R^2\Delta^2\right) & & & \\ & & \frac{1}{3}\left(R^1\Delta^1+R^2\Delta^2+R^3\Delta^3\right) & & \\ & & & \frac{1}{3}\left(R^2\Delta^2+R^3\Delta^3\right) & \\ & & & & \frac{1}{3}R^3\Delta^3 \end{bmatrix} \end{array},$$

and

$$
\begin{array}{cc}
 & \begin{array}{ccccc} 1 & 2 & 3 & 4 & 5 \end{array} \\
\underline{\underline{\alpha}} = \begin{array}{c} 1 \\ 2 \\ 3 \\ 4 \\ 5 \end{array} &
\begin{bmatrix}
\frac{1}{2}\left(\alpha L\right)_{13} & & & & \\
 & & & & \\
 & & \frac{1}{2}\left[\left(\alpha L\right)_{31}+\left(\alpha L\right)_{35}\right] & & \\
 & & & & \\
 & & & & \frac{1}{2}\left(\alpha L\right)_{53}
\end{bmatrix}
\end{array}
$$

Finally, the $\underline{B}$ vector, which contains all terms that do not multiply $\hat{\underline{h}}$ or $d\hat{\underline{h}}/dt$, is

$$
\underline{B} = \begin{array}{c} 1 \\ 2 \\ 3 \\ \\ 4 \\ 5 \end{array}
\begin{bmatrix}
\frac{1}{3}R^1\Delta^1H_1 + \frac{1}{3}W^1\Delta^1 + \frac{1}{2}\left(q_BL\right)_{12} + \frac{1}{2}\left(q_BL\right)_{13} + \frac{1}{2}\left(\alpha L\right)_{13}H_{B1} \\
\frac{1}{3}\left(R^1\Delta^1 + R^2\Delta^2\right)H_2 + \frac{1}{3}\left(W^1\Delta^1 + W^2\Delta^2\right) + \frac{1}{2}\left(q_BL\right)_{21} \\
\frac{1}{3}\left(R^1\Delta^1 + R^2\Delta^2 + R^3\Delta^3\right)H_3 + \frac{1}{3}\left(W^1\Delta^1 + W^2\Delta^2 + W^3\Delta^3\right) + \frac{1}{2}\left[\left(q_BL\right)_{31} + \left(q_BL\right)_{35}\right] \\
+ \frac{1}{2}\left[\left(\alpha L\right)_{31} + \left(\alpha L_{35}\right)\right]H_{B3} \\
\frac{1}{3}\left(R^2\Delta^2 + R^3\Delta^3\right) + \frac{1}{3}\left(W^2\Delta^2 + W^3\Delta^3\right) + Q_1 \\
\frac{1}{3}R^3\Delta^3 + \frac{1}{3}W^3\Delta^3 + \frac{1}{2}\left(q_BL\right)_{53} + \frac{1}{2}\left(\alpha L\right)_{53}H_{B5}
\end{bmatrix},
$$

and vectors $d\hat{\underline{h}}/dt$ and $\hat{\underline{h}}$ are

$$
\frac{d\hat{\underline{h}}}{dt} = \begin{array}{c} 1 \\ 2 \\ 3 \\ 4 \\ 5 \end{array}
\begin{bmatrix} d\hat{h}_1/dt \\ d\hat{h}_2/dt \\ d\hat{h}_3/dt \\ d\hat{h}_4/dt \\ d\hat{h}_5/dt \end{bmatrix}
\text{ and } \hat{\underline{h}} = \begin{array}{c} 1 \\ 2 \\ 3 \\ 4 \\ 5 \end{array}
\begin{bmatrix} \hat{h}_1 \\ \hat{h}_2 \\ \hat{h}_3 \\ \hat{h}_4 \\ \hat{h}_5 \end{bmatrix}.
$$

The final set of equations corresponding to equation (45) can be written

$$\int_0^{\Delta t_{n+1}} \sigma_{n+1}\left[C_{11}\frac{d\hat{h}_1}{dt} + A_{11}\hat{h}_1 + A_{12}\hat{h}_2 + A_{13}\hat{h}_3 - B_1\right]dt' = 0$$

$$\int_0^{\Delta t_{n+1}} \sigma_{n+1}\left[C_{22}\frac{d\hat{h}_2}{dt} + A_{21}\hat{h}_1 + A_{22}\hat{h}_2 + A_{23}\hat{h}_3 + A_{24}\hat{h}_4 - B_2\right]dt' = 0$$

$$\int_0^{\Delta t_{n+1}} \sigma_{n+1}\left[C_{33}\frac{d\hat{h}_3}{dt} + A_{31}\hat{h}_1 + A_{32}\hat{h}_2 + A_{33}\hat{h}_3 + A_{34}\hat{h}_4 + A_{35}\hat{h}_5 - B_3\right]dt' = 0$$

$$\int_0^{\Delta t_{n+1}} \sigma_{n+1}\left[C_{44}\frac{d\hat{h}_4}{dt} + A_{42}\hat{h}_2 + A_{43}\hat{h}_3 + A_{44}\hat{h}_4 + A_{45}\hat{h}_5 - B_4\right]dt' = 0$$

$$\int_0^{\Delta t_{n+1}} \sigma_{n+1}\left[C_{55}\frac{d\hat{h}_5}{dt} + A_{53}\hat{h}_3 + A_{54}\hat{h}_4 + A_{55}\hat{h}_5 - B_5\right]dt' = 0$$

where terms involving zero coefficients were omitted and an entry A_{ij} is $A_{ij} = G_{ij} + R_{ij} + \alpha_{ij}$.

There are no specified-head nodes in figure 6. If node 2 (for example) is designated as a specified-head node, then the second equation above is replaced by $\int_0^{\Delta t_{n+1}} \sigma_{n+1}\left[\hat{h}_2 - H_{B2}\right]dt' = 0$ and $\hat{h}_2$ is replaced by H_{B2} in the remaining equations, i = 1,3,4, and 5, so that the terms $A_{i2}H_{B2}$ are regarded as knowns. To accomplish this, (1) all entries in row 2 and column 2 of matrices $\underline{\underline{G}}$, $\underline{\underline{C}}$, $\underline{\underline{R}}$, and $\underline{\underline{\alpha}}$ are set to zero except for entry (2,2) in matrix $\underline{\underline{\alpha}}$, which is set to unity, (2) row 2 in $\underline{B}$ is set to H_{B2}, and (3) all other rows i = 1,3,4, and 5 in $\underline{B}$ have $A_{i2}H_{B2}$ subtracted from them.

Evaluation of time integral

Time integration of equation (45) is performed using a formula that is analogous to equation (25):

$$\int_0^{\Delta t_{n+1}} \left(\sigma_n\right)^p \left(\sigma_{n+1}\right)^q \, dt' = \frac{p!q!}{(p+q+1)!}\,\Delta t_{n+1}. \tag{52}$$

The simplest solution of equation (45) is obtained when coefficient matrices $\underline{\underline{C}}$ and $\underline{\underline{A}}$ and known vector $\underline{B}$ are constant in time. In this case, term by term integration of equation (45) yields

$$\int_0^{\Delta t_{n+1}} C_{ii} \frac{d\hat{h}_i}{dt} \sigma_{n+1} dt' = C_{ii} \int_0^{\Delta t_{n+1}} \left(\hat{h}_{i,n} \frac{d\sigma_n}{dt} + \hat{h}_{i,n+1} \frac{d\sigma_{n+1}}{dt} \right) \sigma_{n+1} dt'$$

$$= \frac{1}{2} C_{ii} \left(\hat{h}_{i,n+1} - \hat{h}_{i,n} \right), \tag{53}$$

$$\int_0^{\Delta t_{n+1}} A_{ij} \hat{h}_j \sigma_{n+1} dt' = A_{ij} \int_0^{\Delta t_{n+1}} \left(\hat{h}_{i,n} \sigma_n + \hat{h}_{i,n+1} \sigma_{n+1} \right) \sigma_{n+1} dt'$$

$$= \Delta t_{n+1} A_{ij} \left(\frac{1}{6} \hat{h}_{i,n} + \frac{1}{3} \hat{h}_{i,n+1} \right), \tag{54}$$

$$\int_0^{\Delta t_{n+1}} B_i \sigma_{n+1} dt' = B_i \int_0^{\Delta t_{n+1}} \sigma_{n+1} dt' = \frac{1}{2} \Delta t_{n+1} B_i. \tag{55}$$

Therefore, equation (45) is evaluated as

$$\underline{\underline{C}} \left(\hat{\underline{h}}_{n+1} - \hat{\underline{h}}_n \right) + \Delta t_{n+1} \underline{\underline{A}} \left(\frac{1}{3} \hat{\underline{h}}_n + \frac{2}{3} \hat{\underline{h}}_{n+1} \right) = \Delta t_{n+1} \underline{B}. \tag{56}$$

Solution of equation (56) produces round-off errors, which can be reduced by solving for a change in head between time levels rather than for the actual head values, $\hat{h}_{i,n+1}$. By defining $\underline{\delta}$ as 2/3 of the total head change between two time levels and substituting this into equation (56), a convenient equation for solution results. Thus, by defining

$$\underline{\delta} = \frac{2}{3} \left(\hat{\underline{h}}_{n+1} - \hat{\underline{h}}_n \right), \tag{57}$$

$\hat{\underline{h}}_{n+1} = \frac{3}{2} \underline{\delta} + \hat{\underline{h}}_n$ and equation (56) can be written in the form

$$\left(\frac{\underline{\underline{C}}}{(2/3) \Delta t_{n+1}} + \underline{\underline{A}} \right) \underline{\delta} = \underline{B} - \underline{\underline{A}} \hat{\underline{h}}_n. \tag{58}$$

Further reduction of round-off error is obtained by writing the diagonal terms of $\underline{\underline{G}}$ using equation (43) so that $\underline{\underline{G}} \hat{\underline{h}}_n$ can be written in terms of head differences of the form of equations (41) and (42).

Equations (57) and (58) are used to solve for head vectors $\hat{\underline{h}}_{n+1}$ at all time levels successively, starting with n = 0 at which $\underline{h}_0$ is the known initial condition. First, equation (58) is solved for $\underline{\delta}$ using one of the matrix solution routines discussed further on, and second, equation (57) is solved for $\hat{\underline{h}}_{n+1}$, which becomes $\hat{\underline{h}}_n$ for the next time level.

The finite-element in time method given by equation (56) is equivalent to the weighted finite-difference in time method,

$$\underset{=}{C}\left(\hat{\underset{-}{h}}_{n+1} - \hat{\underset{-}{h}}_{n}\right) + \Delta t_{n+1}\, \underset{=}{A}\left[(1-\theta)\hat{\underset{-}{h}}_{n} + \theta\hat{\underset{-}{h}}_{n+1}\right] = \Delta t_{n+1}\underset{-}{B}, \tag{59}$$

with weighting factor θ equal to 2/3. The weighted finite-difference in time method is unconditionally stable for $\theta \geq 1/2$ (Smith, 1965, p. 23-24), but Briggs and Dixon's (1968) criterion shows that use of $\theta<1$ can cause oscillatory solutions if Δt_{n+1} is too large. Bettencourt and others (1981) reported very good accuracy and only slight oscillations in a solution obtained with the finite-element in time method (θ = 2/3). In contrast, their solution to the same problem obtained with the well-known Crank-Nicolson method (θ = 1/2) (Crank and Nicolson, 1947) exhibited large oscillations with little, if any, improvement in overall accuracy over the finite-element in time method. Numerical experiments conducted by the author also show that solutions are accurate and exhibit minimal oscillatory behavior if the sizes of time elements are not too large (which is problem dependent).

Time variability of $\underset{-}{B}$ results if source-bed heads H, specified heads H_B, areal recharge W, or specified boundary flux q_B change with time. A simple method of approximating this time dependence in the finite-element equations is to assume linear time variability during each time element so that during time-element n+1

$$B_i = B_{i,n}\sigma_n + B_{i,n+1}\sigma_{n+1}. \tag{60}$$

Thus, equation (55) is replaced with

$$\int_0^{\Delta t_{n+1}} B_i\sigma_{n+1}dt' = \int_0^{\Delta t_{n+1}} \left(B_{i,n}\sigma_n + B_{i,n+1}\sigma_{n+1}\right)\sigma_{n+1}dt'$$

$$= \frac{1}{6}\Delta t_{n+1}\left(B_{i,n} + 2B_{i,n+1}\right) = \frac{1}{2}\Delta t_{n+1}\bar{B}_i, \tag{61}$$

where $\bar{B}_i$ is a weighted average value of B_i over timespan Δt_{n+1}, defined by

$$\bar{B}_i = \frac{1}{3}\left(B_{i,n} + 2B_{i,n+1}\right). \tag{62}$$

Hence, time dependence of known heads and fluxes may be incorporated into equation (58) by replacing $\underset{-}{B}$ with $\bar{\underset{-}{B}}$.

Time variability of $\underset{=}{C}$, $\underset{=}{A}$, and $\underset{-}{B}$ also results from processes such as unconfined flow, conversions from confined to unconfined flow (and vice versa), nonlinearity of stream-aquifer interactions, and discharges from springs, drains, or evapotranspiration. These types of time variabilities are treated in the sections covering these topics.

Mass-balance calculation

A mass balance based on equation (56) is needed to allow hydrologic budget analysis of the model and to assess the accuracy of the matrix solution methods discussed further on. Total quantities of water moved during the timespan Δt_{n+1} are computed according to equation (61) as the product of weighted average discharges and Δt_{n+1}. To compute these totals, the mass-balance equations are formulated in terms of weighted average discharges and weighted average head, defined as

$$\bar{h} = \frac{1}{3}\hat{h}_n + \frac{2}{3}\hat{h}_{n+1}. \tag{63}$$

By employing equations (56), (62), and (63), along with the definitions of the quantities in these equations, the system of nodal mass-balance equations is written as

$$\frac{1}{2}\sum_{e_i} S^e\Delta^e\left(\bar{h}_i - \hat{h}_{i,n}\right) - \frac{1}{3}\sum_{e_i} R^e\Delta^e\left(\bar{H}_i - \bar{h}_i\right)\Delta t_{n+1} - \frac{1}{3}\sum_{e_i} \bar{W}^e\Delta^e\Delta t_{n+1} - \sum_{e_i} \bar{P}_i^e\Delta t_{n+1}$$

$$- \sum_{\substack{j=1 \\ i\neq j}}^{N} \sum_{e_i} g_{ij}^e\left(\bar{h}_j - \bar{h}_i\right)\Delta t_{n+1} - \bar{Q}_{Bi}\Delta t_{n+1} - \frac{1}{2}\sum_{j'}\left[\left(\bar{q}_B L\right)_{ij'}\right.$$

$$\left. + \left(\alpha L\right)_{ij'}\left(\bar{H}_{Bi} - \bar{h}_i\right)\right]\Delta t_{n+1} \approx 0, \; i = 1,2,\cdots,N, \tag{64}$$

where $\bar{Q}_{Bi} = 0$ unless node i is a specified-head node, in which case $\bar{Q}_{Bi}$ is the volumetric discharge across the node (positive for inflow) obtained by direct solution of equation (64) for $\bar{Q}_{Bi}$. Bars over quantities in equation (64) indicate weighted averages over time.

To obtain the total mass balance over the flow domain, equation (64) is summed over i. When this is done, it can be seen that

$$\sum_{i=1}^{N} \sum_{\substack{j=1 \\ i\neq j}}^{N} \sum_{e_i} g_{ij}^e\left(\bar{h}_j - \bar{h}_i\right) = 0,$$

because $g_{ij}^e = g_{ji}^e$ so that $g_{ij}^e\left(\bar{h}_j - \bar{h}_i\right) + g_{ji}^e\left(\bar{h}_i - \bar{h}_j\right) = 0$. Thus, the components that should sum to give nearly zero are:

Total depletion or accretion of water in storage $= \frac{1}{2}\sum_{i=1}^{N}\sum_{e_i} S^e\Delta^e\left(\bar{h}_i - \hat{h}_{i,n}\right)$.

Total leakage across confining units $= \frac{1}{3}\sum_{i=1}^{N}\sum_{e_i} R^e\Delta^e\left(\bar{H}_i - \bar{h}_i\right)\Delta t_{n+1}$.

Total areal recharge or discharge $= \frac{1}{3}\sum_{i=1}^{N}\sum_{e_i} \bar{W}^e\Delta^e\Delta t_{n+1}$.

Total water pumped into or out of wells $= \sum_{i=1}^{N} \sum_{e_i} \bar{P}_i^e \Delta t_{n+1} = \sum_{j=1}^{P} \bar{Q}_j \Delta t_{n+1}.$

Total water crossing specified-head boundaries $= \sum_{i=1}^{N} \bar{Q}_{Bi} \Delta t_{n+1}.$

Total water crossing Cauchy-type boundaries

$$= \frac{1}{2} \sum_{i=1}^{N} \sum_{j}{}' \left[\left(\bar{q}_B L \right)_{ij'} + \left(\alpha L \right)_{ij'} \left(\bar{H}_{Bi} - \bar{h}_i \right) \right] \Delta t_{n+1}.$$

Average volumetric flow rates in time element n+1 can be obtained by dividing the components by Δt_{n+1}, and running totals over time can be obtained by summing the components over all preceding time elements. The mass imbalance in time element n+1 is obtained by summing the components, and a running mass imbalance is obtained by summing mass imbalances over all preceding time elements.

EXTENSIONS OF THE BASIC EQUATIONS

Unconfined flow

When equation (1) is applied to areal flow in an unconfined aquifer by using the Dupuit approximation (Bear, 1979, p. 111-114), transmissivities are functions of the current saturated thickness of the aquifer, as follows:

$$\begin{aligned} T &= Kb \\ &= K\left(h - z_b\right), \end{aligned} \tag{65}$$

where b is the saturated thickness $h - z_b$ of the aquifer, h is the elevation of the water table above some datum, z_b is the elevation of the aquifer bottom referred to the same datum, and subscripts $\bar{x}$ and $\bar{y}$ were omitted from T and K for simplicity. Because b is head dependent and varies in time, equation (1) is nonlinear, with transmissivities that are head dependent and vary in time.

Time variance of the transmissivities can be handled in the same manner as time variance of B_i. That is, the G_{ij} coefficients, which contain the transmissivities, can be written for time element n+1 as

$$G_{ij} = G_{ij,n}\sigma_n + G_{ij,n+1}\sigma_{n+1}, \tag{66}$$

so that, by using the relationship $A_{ij} = G_{ij} + V_{ij}$, equation (54) is replaced with

$$\int_0^{\Delta t_{n+1}} A_{ij} \hat{h}_j \sigma_{n+1} dt'$$